JCTC Journal of Chemical Theory and Computation

Article

Cite This: J. Chem. Theory Comput. 2018, 14, 5446−5458

pubs.acs.org/JCTC

Wigner Distribution by Adiabatic Switching in Normal Mode or Cartesian Coordinates and Molecular Applications

Amartya Bose[†] and Nancy Makri*[,†,‡]

[†]Department of Chemistry, University of Illinois, Urbana, Illinois 61801, United States

[‡]Department of Physics, University of Illinois, Urbana, Illinois 61801, United States

ABSTRACT: We recently presented a simple, classical trajectory-based method for generating the Wigner phase space density using classical trajectories evolving under an adiabatically switched potential. The adiabatically switched Wigner (ASW) distribution is an approximation to the exact Wigner function, which was found to be highly accurate on model systems. In this paper we discuss the implementation of the ASW procedure to polyatomic molecules both in normal mode coordinates and in Cartesian coordinates. We present its application to a six-degree-of-freedom model based on an *ab initio* quartic potential energy surface developed for formaldehyde in the normal mode representation and for butyne in Cartesian coordinates using the CHARMM force field. Comparisons of equilibrium properties against accurate quantum mechanical results indicate that the ASW is reliable and highly accurate over a wide temperature range in both the coordinate systems. Further, the ASW density is invariant under classical evolution, thus it is ideally suited to quasiclassical trajectory simulations. We also describe a very simple ASW-based procedure for obtaining complex-valued quasiclassical time correlation functions and vibrational spectra.

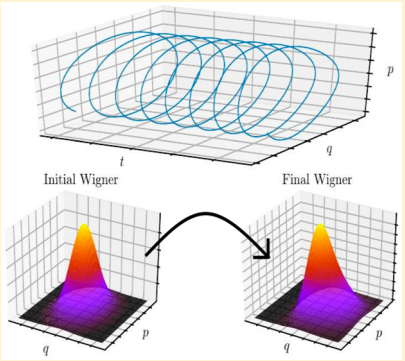

I. INTRODUCTION

The exponential scaling of quantum mechanics has sparked the development of a plethora of approximate methods for studying the equilibrium and dynamical properties of polyatomic systems. Classical mechanics has a prominent place in this regard. The computational cost of obtaining Newtonian trajectories is relative low and scales very favorably with the number of degrees of freedom. Semiclassical approximations can account for important quantum effects semiquantitatively through classical trajectories, and even purely classical molecular dynamics (MD) simulations can adequately capture many properties of condensed phase and biological systems.

The major drawback of MD simulations is the absence of quantization of the thermal density matrix and the neglect of zero-point energy (ZPE). The latter can be very substantial for high-frequency molecular vibrations and can result in significant broadening of the Boltzmann distribution. In order to account for such quantum effects, it becomes essential to incorporate quantization in the phase space density from which trajectory initial conditions will be sampled. This is usually achieved by means of the Wigner prescription,[1] which can also be derived by linearizing the semiclassical initial value representation[2] or the path integral expression.[3] In these, the phase space function is obtained via the Wigner transform of the initial density matrix. The Wigner density is also required in methods that employ quantum-classical Liouville dynamics.[4]

For a system of one degree of freedom, the Wigner transform of a density operator $\hat{\rho}$ is given by the integral

$$W(x_0, p_0) = \frac{1}{\sqrt{2\pi\hbar}} \int_{-\infty}^{\infty} \left\langle x_0 + \frac{1}{2}\Delta x \middle| \hat{\rho} \middle| x_0 - \frac{1}{2}\Delta x \right\rangle e^{-ip_0\Delta x/\hbar} d\Delta x \tag{1.1}$$

The oscillatory Fourier-like integrand makes the evaluation of the Wigner density a challenging task for systems of many degrees of freedom, as Monte Carlo methods[5] encounter a severe "sign problem" and thus do not converge efficiently. When the use of a quantized phase space density is necessary, it is common practice to use the Wigner distribution that corresponds to the harmonic fit to the Hamiltonian. Approximate procedures for constructing the Wigner density of anharmonic systems include local[6] and variationally optimized[3] Gaussian approximations and the thermal Gaussian approximation,[7] which is based on the dynamics of frozen Gaussians[8] in imaginary time. Extensions of the thermal Gaussian approximation which capture quantum corrections[9] have also been proposed. In the special case of a system coupled to a harmonic bath, the quasi-adiabatic propagator path integral[10] has been employed to develop a numerically exact treatment of the bath Wigner density.[11]

We have recently described[12] a very simple, approximate method for obtaining the Wigner transform of the density operator corresponding to a thermal Boltzmann density using the classical adiabatic theorem.[13] Starting from a suitable zeroth-order Hamiltonian for which the Wigner density is either analytically or numerically available, the phase space distribution is propagated in time via classical trajectories,

Received: February 26, 2018
Published: October 10, 2018

DOI: 10.1021/acs.jctc.8b00179
J. Chem. Theory Comput. 2018, 14, 5446−5458

while the potential is slowly transformed to that of the target Hamiltonian. A series of tests on one-dimensional models and a system-bath Hamiltonian showed that the adiabatically switched Wigner (ASW) density is not only easy to obtain but also quite accurate. Further, the ASW procedure is ideally suited to propagation via classical trajectories and has the desirable property of being preserved under classical dynamics.

In the present paper we demonstrate the use of the ASW method for treating intramolecular vibrations either in the normal mode representation or in Cartesian coordinates. Normal mode coordinates provide an excellent starting point for ASW calculations, since they lead to an obvious, physically relevant quadratic reference Hamiltonian whose Wigner density is readily available. Cartesian coordinates are convenient and often preferred in large molecular systems. We illustrate the procedure and assess its accuracy by applying it to a model based on the *ab initio* quartic potential energy surface developed for formaldehyde[14] and the CHARMM force field for the butyne molecule in Cartesian coordinates. We assess the accuracy of the ASW density by evaluating various thermodynamic properties, which are compared to the results of fully quantum mechanical path integral Monte Carlo[15] (PIMC) calculations. The ASW results are also compared to those obtained using the classical Boltzmann distribution and to quantum mechanical results within a quadratic approximation. We also illustrate an extremely easy implementation of the ASW procedure to obtain complex-valued quasiclassical time correlation functions and vibrational spectra.

Section II reviews the ASW method and discusses its implementation in normal mode coordinates and also in Cartesian coordinates. Section III presents the implementation of the method on equilibrium and dynamical properties of formaldehyde and presents comparisons against fully quantum mechanical results as well as classical, semiclassical, and quadratic approximations. Section IV shows the results of applying the method to butyne described by the CHARMM force field. Some concluding remarks are given in section V.

II. ADIABATICALLY SWITCHED WIGNER DENSITY

II.1. Summary of the Procedure. Consider a system described by the Hamiltonian $H(\mathbf{q},\mathbf{p})$, where $\mathbf{q}$ is the vector containing the n (orthogonal) coordinates and $\mathbf{p}$ are the conjugate momenta. The procedure begins by identifying a zeroth-order Hamiltonian H_0 for which the Wigner function $W^{(0)}$ is known, either analytically or numerically. A convenient choice for H_0 is often the quadratic part of the Hamiltonian in normal mode coordinates.

Once the zeroth-order Hamiltonian has been identified, one uses a Monte Carlo procedure to sample phase space points from the chosen zeroth-order Wigner distribution. Each of these phase space points is subsequently used to launch a classical trajectory, which is propagated under a slowly varying Hamiltonian that is initially given by H_0 and which is gradually modified by including the remaining potential terms, such that eventually it becomes the target Hamiltonian H. The applications reported in this paper used a switching function of the form[23]

$$s(t) = \frac{t}{\tau} - \frac{1}{2\pi}\sin\left(2\pi\frac{t}{\tau}\right) \tag{2.1}$$

This function is a sigmoidal transfer function which goes from 0 to 1 over the time period of τ.

According to the classical adiabatic theorem, a trajectory that lies on a phase space torus evolves in such a manner so as to maintain a constant action, as long as the anharmonic terms are switched on infinitely slowly. However, the energy of the trajectory changes during the adiabatic switching process. To account for the change in the Boltzmann population, we adjust the weight of each trajectory by a rescaling factor f, i.e.

$$W(\mathbf{q},\mathbf{p}) = \kappa W^{(0)}(\mathbf{q}_0,\mathbf{p}_0) f(\mathcal{E}^{(0)},\mathcal{E}) \tag{2.2}$$

where κ is a normalization factor that does not need to be determined. In particular, we have shown[12] that the following rescaling factor

$$f_{\mathrm{ZPE}}(\mathcal{E}^{(0)},\mathcal{E}) = \exp\left(-\tanh(\beta E_0)\frac{\mathcal{E}(\mathbf{q},\mathbf{p})}{E_0} + \tanh(\beta E_0^{(0)})\frac{\mathcal{E}^{(0)}(\mathbf{q}_0,\mathbf{p}_0)}{E_0^{(0)}}\right) \tag{2.3}$$

leads to an excellent approximation of the Wigner density. Here $\mathcal{E}^{(0)}(\mathbf{q}_0,\mathbf{p}_0)$ is the initial energy of a classical trajectory with phase space coordinates $\mathbf{q}_0,\mathbf{p}_0$, sampled from the Wigner distribution corresponding to the harmonic reference Hamiltonian, $\mathcal{E}(\mathbf{q},\mathbf{p})$ is the energy reached at the end of the adiabatic switching process, and $E_0^{(0)}$ and E_0 are the zero-point energies (ZPE) of the reference and full Hamiltonians, respectively. At high temperatures, eq 2.3 becomes the ratio of the classical Boltzmann factors at the initial and final energies, ensuring the correct high temperature limit of the Wigner distribution. At low temperatures, it produces (by construction) the appropriate quantum mechanical scaling factor for the harmonic oscillator.[12] If the Hamiltonian is sufficiently quadratic near the potential minimum, this procedure results in an ASW distribution which faithfully resembles the Wigner phase space density of the full Hamiltonian.

Calculation of the ZPE, while possible (e.g., via quantum Monte Carlo methods[16]), is impractical for multidimensional anharmonic systems. However, typical molecular systems are nearly harmonic at the energy of the ground vibrational state. In such situations the harmonic ZPE provides a simple and sufficiently accurate approximation to E_0. If the harmonic approximation to the ZPE is not adequate, it may be improved (with minimal computational cost) by adding the diagonal anharmonicity to the harmonic reference Hamiltonian. For the calculations presented in this paper the use of the harmonic ZPE in the rescaling factor was sufficiently accurate.

A general issue with quasiclassical propagation methods is the inconsistency between the initial quantum density and the classical dynamics that follows. This inconsistency manifests itself in the loss of temporal invariance of thermal distributions and thermodynamic quantities. Improved dynamical procedures that partially overcome this issue are available,[17] although such schemes are computationally expensive. In this regard, a significant benefit of the ASW method is that the obtained phase space density remains (by construction) invariant. We demonstrate this property for the multidimensional normal mode system studied here.

Last, we note in this section that the zeroth-order Hamiltonian does not have to be quadratic. Another possibility is to use a separable, anharmonic Hamiltonian and construct

DOI: 10.1021/acs.jctc.8b00179
J. Chem. Theory Comput. 2018, 14, 5446−5458

the Wigner function for each degree of freedom through an inexpensive basis set calculation.

II.2. Quasiclassical Time Correlation Functions and Spectra. One of the most common uses of the Wigner function is for generating time correlation functions via classical molecular dynamics calculations and, through Fourier transformation, molecular spectra. The quantum mechanical autocorrelation function for the coordinate k is given by

$$C_k(t) = \mathrm{Tr}(\hat{\rho}_0 \hat{q}_k(0)\hat{q}_k(t)) \tag{2.4}$$

The "proper" (most accurate) way of obtaining a quasiclassical approximation for this is given by

$$C_k(t) = \int_{-\infty}^{\infty} d\mathbf{q}(0) \int_{-\infty}^{\infty} d\mathbf{p}(0)\tilde{W}(\mathbf{q}(0), \mathbf{p}(0))q_k(t) \tag{2.5}$$

where $\tilde{W}$ is the Wigner transform of the combined operator $\hat{\rho}_0\hat{q}_k$, and the integration variables $\{\mathbf{q}(0),\mathbf{p}(0)\}$ serve as initial conditions of classical trajectories that reach the phase space point $\{\mathbf{q}(t),\mathbf{p}(t)\}$. Rather than performing the adiabatic switching for this modified density, we observe that

$$\begin{aligned}\tilde{W}(\mathbf{q}, \mathbf{p}) &= (2\pi\hbar)^{-\frac{n}{2}} \int_{-\infty}^{\infty} \left\langle \mathbf{q} + \frac{1}{2}\Delta\mathbf{q}\middle|\hat{\rho}_0\hat{q}_k\middle|\mathbf{q} - \frac{1}{2}\Delta\mathbf{q}\right\rangle e^{-i\mathbf{p}\cdot\Delta\mathbf{q}/\hbar} d\Delta\mathbf{q} \\ &= (2\pi\hbar)^{-\frac{n}{2}} \int_{-\infty}^{\infty} \left\langle \mathbf{q} + \frac{1}{2}\Delta\mathbf{q}\middle|\hat{\rho}_0\middle|\mathbf{q} - \frac{1}{2}\Delta\mathbf{q}\right\rangle \\ &\quad \left(q_k - \frac{1}{2}\Delta q_k\right) e^{-i\mathbf{p}\cdot\Delta\mathbf{q}/\hbar} d\Delta\mathbf{q} \\ &= q_k W(\mathbf{q}, \mathbf{p}) - \frac{1}{2} i\hbar \frac{\partial}{\partial p_k} W(\mathbf{q}, \mathbf{p})\end{aligned} \tag{2.6}$$

It follows that

$$\int_{-\infty}^{\infty} d\mathbf{q}(0) \int_{-\infty}^{\infty} d\mathbf{p}(0) W(\mathbf{q}(0), \mathbf{p}(0))q_k(0)q_k(t) = \mathrm{Re}C_k(t) \tag{2.7}$$

i.e., the primitive quasiclassical expression (which is used by some researchers in place of the proper quasiclassical form, eq 2.5), yields the real part of the autocorrelation function. (We note that this is not true in the case of nonlinear operators.) This expression involves the Wigner transform of the ordinary density operator, so one can proceed to implement the ASW procedure. However, eq 2.7 does not give the imaginary part of the correlation function, which can be substantial at low temperatures or for high frequency degrees of freedom.

Spectral information is obtained from the Fourier transformation of time correlation functions

$$G_k(\omega) = \frac{1}{\sqrt{2\pi}} \int_{-\infty}^{\infty} C_k(t) e^{i\omega t} dt \tag{2.8}$$

Even if one is only interested in the real part of the autocorrelation function in the time domain, the imaginary part of $C_k(t)$ must be retained when calculating the spectrum, because it contributes to the Fourier integral. The spectrum can be decomposed into even and odd components

$$G_k(\omega) = G_k^{\mathrm{even}}(\omega) + G_k^{\mathrm{odd}}(\omega) \tag{2.9}$$

which correspond to the real and the imaginary parts of an autocorrelation function

$$G_k^{\mathrm{even}}(\omega) \equiv \int \mathrm{Re}C_k(t) e^{i\omega t} dt, \quad G_k^{\mathrm{odd}}(\omega) \equiv i \int \mathrm{Im}\, C_k(t) e^{i\omega t} dt \tag{2.10}$$

It has been shown[18] that these components are related:

$$G_k^{\mathrm{even}}(\omega) = -\coth\left(\frac{1}{2}\hbar\omega_k\beta\right) G_k^{\mathrm{odd}}(\omega) \tag{2.11}$$

Thus, the spectrum is given by

$$G_k(\omega) = G_k^{\mathrm{even}}(\omega)\left[1 - \tanh\left(\frac{1}{2}\hbar\omega_k\beta\right)\right] \tag{2.12}$$

The quantum mechanical correction arising from the imaginary part of the correlation function leads to distortion of the spectrum. According to eq 2.12, this quantum mechanical effect can be obtained from the primitive quasiclassical expression which involves the Wigner transform of the ordinary density. We note that the inferred odd component of the spectral function, eq 2.12, may be inverse-Fourier transformed to yield the imaginary part of the autocorrelation function.

The Wigner density may be evaluated by the ASW procedure at the end of the required adiabatic switching time τ, the value of the Wigner function $W(\mathbf{q}(\tau),\mathbf{p}(\tau))$. The coordinate values $\mathbf{q}(\tau),\mathbf{p}(\tau)$ define the initial conditions for the dynamical calculation to obtain the correlation function, i.e.

$$\mathrm{Re}C_k(t) = \int_{-\infty}^{\infty} d\mathbf{q}(\tau) \int_{-\infty}^{\infty} d\mathbf{p}(\tau) W(\mathbf{q}(\tau), \mathbf{p}(\tau))q_k(\tau)q_k(\tau + t) \tag{2.13}$$

Using eq 2.2, along with Liouville's theorem, this expression becomes

$$\begin{aligned}&\mathrm{Re}C_k(t) \\ &= \int_{-\infty}^{\infty} d\mathbf{q}(0) \int_{-\infty}^{\infty} d\mathbf{p}(0) W^{(0)}(\mathbf{q}(0), \mathbf{p}(0)) f(\mathcal{E}^{(0)}, \mathcal{E}) q_k(\tau)q_k(\tau + t)\end{aligned} \tag{2.14}$$

which is evaluated by a standard Metropolis Monte Carlo procedure using the zeroth-order Wigner function as the sampling function. Eq 2.14 involves combining the adiabatic switching process with the dynamics of the Hamiltonian of interest in a single calculation. Starting from the phase space point $\mathbf{q}(0),\mathbf{p}(0)$, a classical trajectory is launched, which evolves under the time-dependent adiabatically switched potential. At the time τ the potential anharmonicity has been fully switched on, and the trajectory continues under the full Hamiltonian (which no longer changes). Correlations are obtained from this segment of the trajectory.

II.3. Implementation in Normal Mode Coordinates. Consider a molecular Hamiltonian composed of N atoms, which is expressed in terms of $n = 3N - 6$ (or $3N - 5$) normal mode coordinates $\mathbf{Q}$ and has the general form

$$\hat{H} = \hat{H}_0 + \hat{V} \tag{2.15}$$

where

$$\hat{H}_0 = \sum_{i=1}^{n} \left(\frac{1}{2}\hat{P}_i^2 + f_{ii}\hat{Q}_i^2\right) \tag{2.16}$$

$$V(\mathbf{Q}) = \sum_{i,j,k}^{n} f_{ijk} Q_i Q_j Q_k + \sum_{i,j,k,l}^{n} f_{ijkl} Q_i Q_j Q_k Q_l \tag{2.17}$$

Here $f_{ii} = \frac{1}{2}\omega_i^2$ (where ω_i are the normal-mode frequencies), and f_{ijk} and f_{ijkl} are cubic and quartic anharmonicity coefficients, respectively, obtained from the potential function fit. Since the Hamiltonian is expressed in normal modes, the

DOI: 10.1021/acs.jctc.8b00179
J. Chem. Theory Comput. 2018, 14, 5446−5458

Table 1. Force Constants (in Atomic Units) for the Modified, Bound Model of the Formaldehyde Normal Mode Vibrations

i, j, k, l	force constant	i, j, k, l	force constant	i, j, k, l	force constant
1 1	8.95641e-5	1 2 2 2	6.06809e-10	2 3 3 3	5.79834e-11
2 2	3.28072e-5	1 2 2 3	3.49433e-9	2 3 4 4	8.16788e-10
3 3	2.47445e-5	1 2 3 3	3.41881e-9	2 3 5 5	2.49993e-8
4 4	1.46576e-5	1 2 4 4	3.99302e-9	2 3 5 6	8.88722e-9
5 5	9.41724e-5	1 2 5 5	1.23419e-8	2 3 6 6	1.92595e-9
6 6	1.67271e-5	1 2 5 6	4.33096e-8	3 3 3 3	3.01839e-11
1 1 1	1.58395e-6	1 2 6 6	1.98986e-9	3 3 4 4	2.82284e-10
2 2 2	−3.09488e-7	1 3 3 3	8.19983e-10	3 3 5 5	2.08768e-8
3 3 3	−7.42473e-9	1 3 4 4	3.47055e-9	3 3 5 6	2.63248e-9
1 1 1 1	1.64404e-8	1 3 5 5	1.24585e-8	3 3 6 6	1.54438e-9
1 1 1 2	1.75202e-9	1 3 5 6	7.06454e-8	4 4 4 4	7.72218e-10
1 1 1 3	4.35259e-10	1 3 6 6	2.71959e-9	4 4 5 5	2.78328e-8
1 1 2 2	5.11727e-9	2 2 2 2	2.09690e-9	4 4 5 6	3.41463e-10
1 1 2 3	1.84464e-8	2 2 2 3	2.29151e-9	4 4 6 6	1.43632e-9
1 1 3 3	1.54362e-8	2 2 3 3	1.57200e-9	5 5 5 5	2.03858e-8
1 1 4 4	2.35793e-8	2 2 4 4	5.30463e-10	5 5 5 6	4.41000e-9
1 1 5 5	1.13248e-7	2 2 5 5	8.45341e-9	5 5 6 6	2.01654e-8
1 1 5 6	9.64337e-10	2 2 5 6	1.88770e-9	5 6 6 6	7.36786e-10
1 1 6 6	1.84492e-8	2 2 6 6	1.00897e-10	6 6 6 6	6.16225e-10

quadratic terms are diagonal. Thus, the normal mode representation gives rise to a convenient zeroth-order Hamiltonian, whose Wigner density is available analytically. At a temperature $T = 1/k_B\beta$ (where k_B is the Boltzmann constant), the Wigner function corresponding to H_0 is given by the expression

$$W_0(\mathbf{Q}, \mathbf{P}) = (\hbar\pi)^{-n} \prod_{j=1}^{n} \tanh\left(\frac{1}{2}\hbar\omega_j\beta\right) e^{-\tanh(\frac{1}{2}\hbar\omega_j\beta)(\omega_j Q_j^2/\hbar + P_j^2/\omega_j\hbar)} \tag{2.18}$$

The ASW density is obtained through the following procedure.[12] Phase space coordinates are sampled from the zeroth-order Wigner density via a Monte Carlo[5] random walk. Classical trajectories are launched with initial conditions obtained from the sampled phase space points, while the Hamiltonian is slowly changed from H_0 to the full H over a time length τ according using a switching function $s(t)$, i.e.

$$H(t) = H_0 + s(t)V \tag{2.19}$$

where $s(0) = 0$, and $s(\tau) = 1$. Various forms of the switching function may be used. The switching function used is given after the discussion on the ASW method in Cartesian coordinates.

II.4. Implementation in Cartesian Coordinates. When the Hamiltonian is given in Cartesian coordinates $\mathbf{R} = (\mathbf{r}_1,\cdots,\mathbf{r}_N)$ and $\mathbf{P}$, the starting point is again the normal mode representation of the full Hamiltonian. To obtain the normal modes, the Hamiltonian is expanded through quadratic terms about the potential minimum of a "reference" configuration $\mathbf{R}^{eq} = (\mathbf{r}_1^{eq},...,\mathbf{r}_N^{eq})$. The normal-mode analysis is performed once, and the normal mode vectors, along with the force constant matrix and its eigenvalues, are stored. Given the normal mode coordinates of a phase space point, it is then easy to obtain the corresponding Cartesian coordinates. The zeroth-order Hamiltonian is

$$H_0 = \sum_{j}^{3N-6} \frac{1}{2}P_j^2 + f_{jj}Q_j^2 \tag{2.20}$$

where $\mathbf{Q}$ and $\mathbf{P}$ are again the normal mode coordinates and momenta, which are obtained in terms of the Cartesian variables. For a molecular system, the full Hamiltonian is often given in terms of bond lengths and angles, as well as nonbonded atom interactions. The normal mode coordinates and momenta are functions of the Cartesian variables, and so is $\hat{H}_0$.

During the adiabatic switching process, the Hamiltonian must be slowly changed from H_0 to H over a time period τ

$$H(\mathbf{R}, \mathbf{P}; t) = (1 - s(t))H_0(\mathbf{R}, \mathbf{P}) + s(t)H(\mathbf{R}, \mathbf{P}) \tag{2.21}$$

where $s(t)$ is again the switching function.

The procedure starts by sampling a phase space point in normal mode coordinates from the Wigner density corresponding to H_0. To integrate the classical trajectory, the coordinates of the sampled point are transformed to the Cartesian representation. The forces are calculated using a finite difference method, which requires obtaining the energies at two nearby points. Getting the energies corresponding to the second term involving the CHARMM force field is straightforward. However, obtaining the value of H_0 at the instantaneous phase space point **R**,**P** requires knowledge of the force constant matrix and the coordinate displacements. To minimize numerical error, it is best to reorient the molecule so that the atoms are as close as possible to the reference configuration from which the normal modes were obtained. This is done by using the Eckart frame transformation. This involves the rotation matrix $\mathbf{C}$, which satisfies the rotational Eckart relation[19]

$$\sum_{j=1}^{N} m_j\mathbf{r}_j^{eq} \times (\mathbf{C}\cdot\mathbf{r}_j - \mathbf{r}_j^{eq}) = 0 \tag{2.22}$$

The rotation matrix is determined using the procedure described by described by Czakó and Bowman.[20] Once the Eckart rotation matrix has been found, the normal-mode analysis is now done on the atomic coordinate vectors $(\mathbf{C}\cdot\mathbf{r}_i^{eq} - \mathbf{r}^{eq})$. The force at this point from the zeroth-order Hamiltonian

DOI: 10.1021/acs.jctc.8b00179
J. Chem. Theory Comput. 2018, 14, 5446−5458

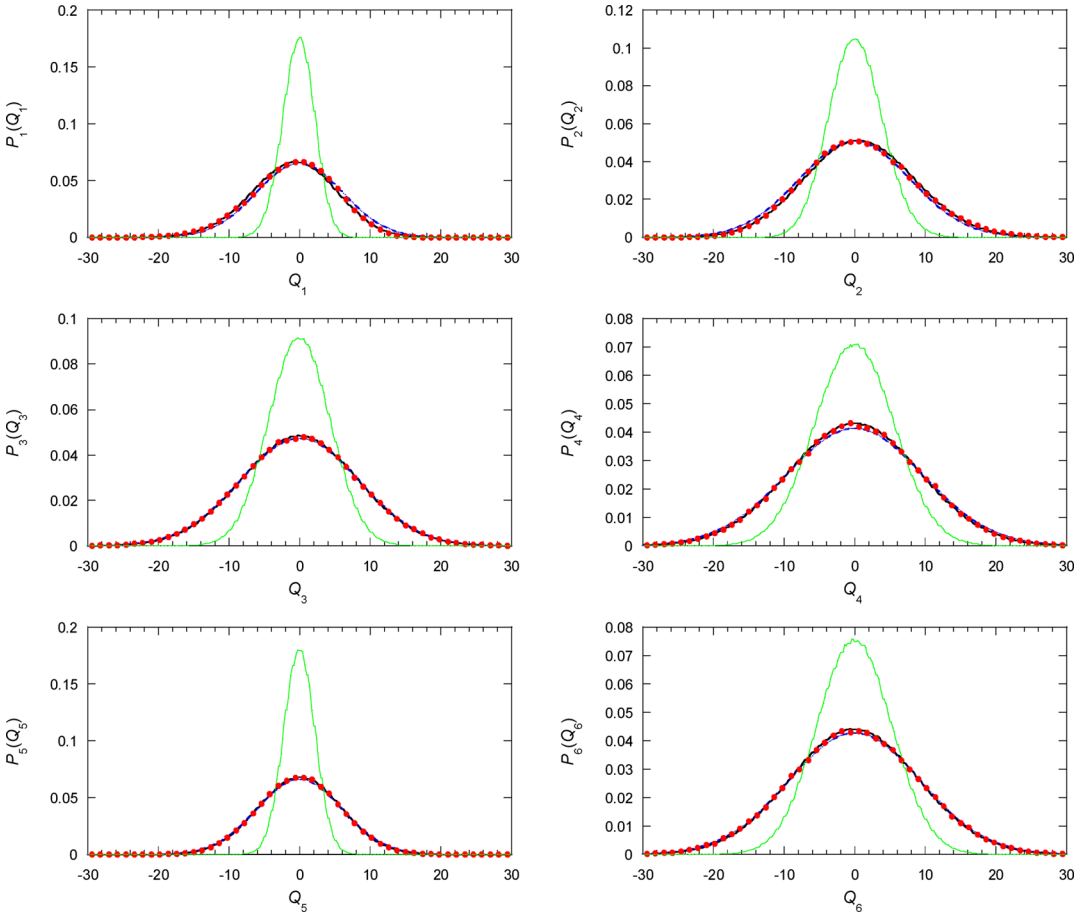

Figure 1. Marginal distributions of the six normal modes at 300 K. At this temperature $\hbar\omega_{min}\beta = 5.70$ and $\hbar\omega_{max}\beta = 14.4$. Black line: PIMC results. Blue dashed lines: harmonic approximation to Wigner density. Green line: classical Boltzmann approximation. Red markers: ASW results.

is added to the force from the full Hamiltonian according to eq 2.21 to obtain the total force on the atoms.

III. APPLICATION TO A MOLECULAR MODEL WITH SIX NORMAL MODES

In this section we apply the ASW to a model based on the *ab initio* quartic potential energy surface developed by Romanowski et al.[14] for the formaldehyde molecule. The normal-mode frequencies are 2937, 1778, 1544, 1188, 3012, and 1269 cm^{-1}. Adiabatic switching has been used to study the low-lying semiclassical eigenstates of this system.[21] Unfortunately, the quartic fit to the potential is unbound and thus ill-behaved at finite temperatures, as it leads to unstable trajectories. We thus modified the potential to a confined form, for which trajectories are stable and bound (even at very high temperatures). Not surprisingly, the confining modification led to small upward shifts of the energy levels and blue shifts in most spectral features. Using the adiabatic switching method[13,22] (which is numerically exact for the ground state energy), we found that the ZPE was increased by 4% and the energy of the first excited state by nearly 5%. The full Hamiltonian has the form given in Equations 2.15−2.17 with $n = 6$, and the modified force constants are given in Table 1.

The anharmonic terms of the Hamiltonian were switched on according to eq 2.1 over a time period of $\tau = 2$ ps. The switching time was chosen to ensure convergence at the highest temperature and kept fixed for all the results reported. We note that much shorter switching times could have been chosen at lower temperatures.

III.1. Equilibrium Properties. To assess the accuracy of the ASW density, we first compare various equilibrium properties to accurate results obtained via PIMC calculations and also against those obtained within the harmonic approximation at various temperatures. Figures 1 and 2 show the marginal distributions

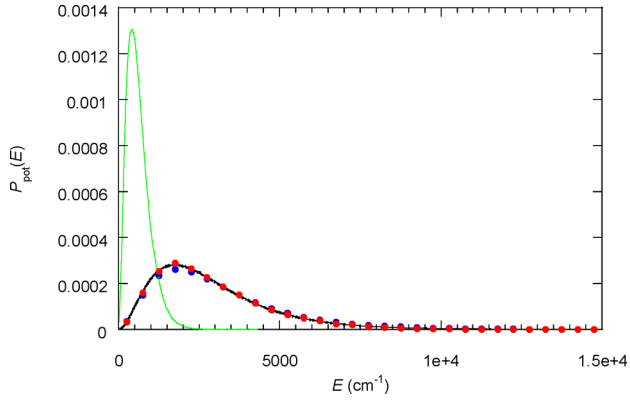

Figure 2. Potential energy distribution function at 300 K. Black line: PIMC results. Blue markers: harmonic approximation to Wigner density. Green line: classical Boltzmann approximation. Red markers: ASW results.

DOI: 10.1021/acs.jctc.8b00179
J. Chem. Theory Comput. 2018, 14, 5446−5458

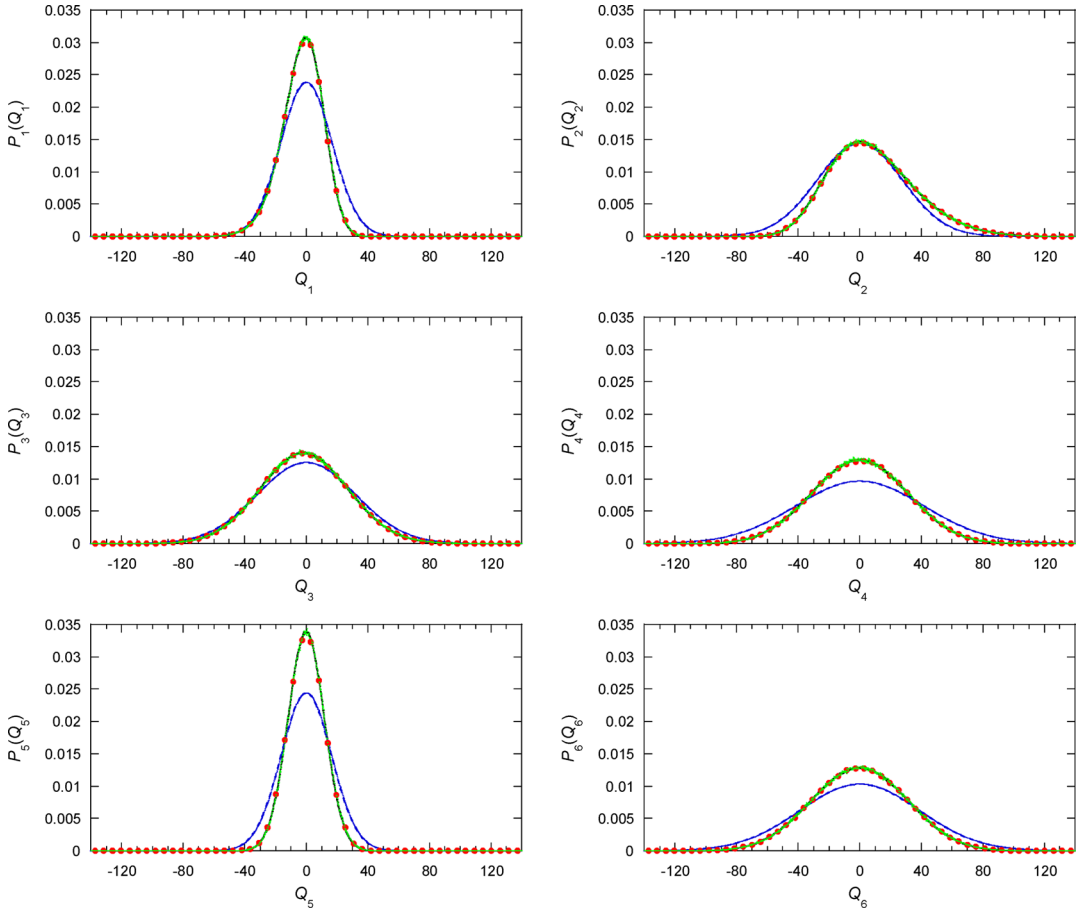

Figure 3. Marginal distributions of the six normal modes at a high temperature such that $\hbar\omega_{min}\beta = 0.11$ and $\hbar\omega_{max}\beta = 0.27$. Black line: PIMC results. Blue dashed lines: harmonic approximation to Wigner density. Green line: classical Boltzmann approximation. Red markers: ASW results.

$$P_i(Q_i) = \int_{-\infty}^{\infty} dQ_1 \cdots \int_{-\infty}^{\infty} dQ_{i-1} \int_{-\infty}^{\infty} dQ_{i+1} \int_{-\infty}^{\infty} dQ_n \int_{-\infty}^{\infty} dP_1 \cdots \int_{-\infty}^{\infty} dP_n W(Q_1, ..., Q_n, P_1, ..., P_n) \quad (3.1)$$

of the normal mode coordinates, as well as the distribution of the total potential energy

$$P_{pot}(E) = \int_{-\infty}^{\infty} dQ_1 \cdots \int_{-\infty}^{\infty} dQ_n \int_{-\infty}^{\infty} dP_1 \cdots \int_{-\infty}^{\infty} dP_n W(Q_1, ..., Q_n, P_1, ..., P_n)\delta(E - V(Q_1, ..., Q_n)) \quad (3.2)$$

at 300 K. All vibrational modes of this molecule are relatively cold at room temperature ($\hbar\omega_i\beta > 5$). As a result, the normal mode distributions shown in Figure 1 are Gaussian-like and in good agreement with those obtained from the harmonic approximation to the Wigner density. Anharmonicity leads to small deviations from the harmonic results. Quantum ZPE effects are very prominent at this temperature. The marginal distributions and potential energy distribution obtained from the classical Boltzmann density are much narrower and shifted compared to the PIMC results. As seen in Figures 1 and 2, the ASW density does an excellent job of capturing these ZPE effects and the small anharmonic corrections.

While neither the original nor the modified potential surface is suitable for high-temperature calculations, the modified potential offers a convenient model for investigating the accuracy of various approximations over a wide range of temperatures. In particular, anharmonicity effects are very prominent at high temperatures, both in the diagonal terms but also in the mode−mode coupling parts of the potential. The results of this comparison have important implications for the performance of these approximate methods on large molecules containing low-frequency vibrations, which are highly excited at physiological temperatures and often strongly anharmonic. Figures 3 and 4 shows the normal mode distributions at a temperature for which $\hbar\omega_{min}\beta = 0.11$ and $\hbar\omega_{max}\beta = 0.27$. The accurate distributions obtained from PIMC calculations are

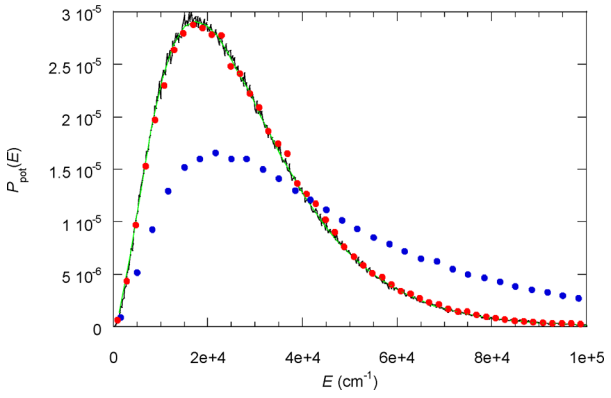

Figure 4. Potential energy distribution function at the temperature specified in Figure 3. Black line: PIMC results. Blue markers: harmonic approximation to Wigner density. Green line: classical Boltzmann approximation. Red markers: ASW results.

DOI: 10.1021/acs.jctc.8b00179
J. Chem. Theory Comput. 2018, 14, 5446−5458

strongly skewed at this temperature and resemble closely the classical Boltzmann distributions. Not surprisingly, the harmonic approximation leads to poor results in this case. The ASW procedure again leads to results that are practically indistinguishable from those obtained through the numerically exact PIMC methodology.

In order to quantify the accuracy of the ASW distribution over a broad temperature range, we report the Hellinger distance of the ASW marginal distribution of each mode from that given by the PIMC calculation, given by

$$g_i^{\mathrm{ASW}} = \left(1 - \int_{-\infty}^{\infty} \sqrt{P_i^{\mathrm{ASW}}(Q_i) P_i^{\mathrm{PIMC}}(Q_i)}\, dQ_i\right)^{1/2} \tag{3.3}$$

The Hellinger distance is a measure of the similarity of two probability distributions. The measure is zero for identical distributions and unity for pairs of distributions that do not overlap. In Figure 5 we compare the Hellinger distance of the

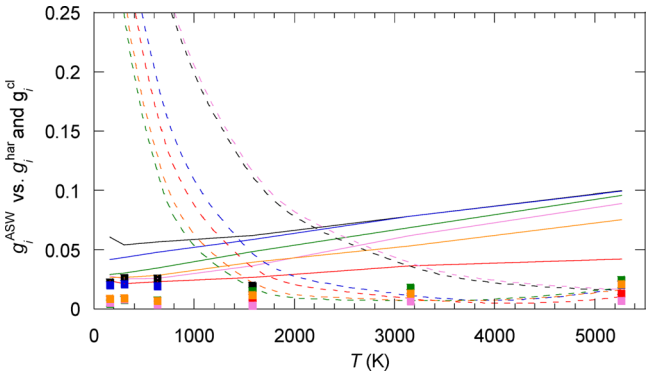

Figure 5. Hellinger distances of the position distributions of the various modes with the PIMC distributions as a function of temperature. Markers: ASW density. Solid lines: harmonic approximation to the Wigner density. Dashed lines: classical Boltzmann density. Black: mode 1. Blue: mode 2. Red: mode 3. Green: mode 4. Purple: mode 5. Orange: mode 6.

ASW distribution from the PIMC result against the Hellinger distance g_i^{har} of the harmonic Wigner density and that of the classical Boltzmann density g_i^{cl}. Not surprisingly, the error of the harmonic approximation to the Wigner density decreases monotonically with increasing temperature, while the classical Boltzmann density fails at low temperatures. The Hellinger distance of the ASW density remains smaller than 0.03 over the entire temperature range considered, including low temperatures with large ZPE effects and very high temperatures where strongly anharmonic potential regions are probed.

Last, we use the Wigner distributions to obtain the expectation values of the squares of the normal mode coordinates

$$\langle Q_i^{\,2}\rangle = \int_{-\infty}^{\infty} dQ_1 \cdots \int_{-\infty}^{\infty} dQ_n \int_{-\infty}^{\infty} dP_1 \cdots \int_{-\infty}^{\infty} dP_n W(Q_1, \ldots, Q_n, P_1, \ldots, P_n) Q_i^{\,2} \tag{3.4}$$

Figure 6 shows the percentage error of $\langle Q_i^2\rangle$ at various temperatures. It is seen that the error of the harmonic approximation grows steeply with temperature. The error resulting from ASW distribution remains small at all temperatures, exhibiting a broad maximum at intermediate temperatures.

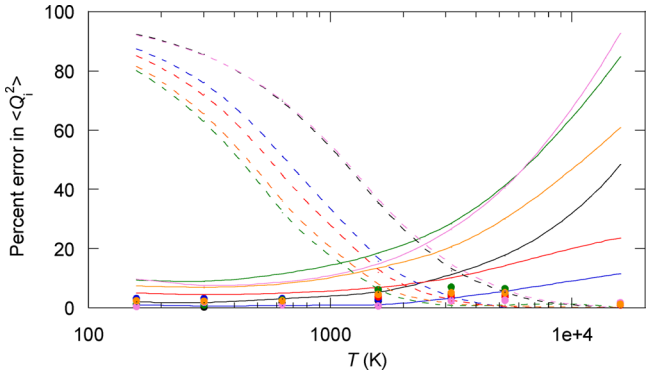

Figure 6. Percent errors in $\langle Q_i^2\rangle$ for the normal mode coordinates as a function of temperature. Solid markers: results from ASW density. Solid lines: results from harmonic approximation to the Wigner density. Dashed lines: results from classical Boltzmann density. Black: mode 1. Blue: mode 2. Red: mode 3. Green: mode 4. Purple: mode 5. Orange: mode 6.

III.2. Dynamical Properties. As discussed earlier, the main appeal of the Wigner density is its use for generating initial conditions for quasiclassical or semiclassial trajectory simulations. In the last part of this section we study the evolution of the ASW density under classical dynamics, as well as time-dependent observables and the resulting frequency-domain spectra.

First we examine the temporal invariance of thermodynamic quantities. Figure 7 shows the average potential energy as a function of time at two temperatures. It is seen that this quantity remains constant, as the ASW-generated Wigner density remains invariant under classical propagation. This stability, a consequence of the classical procedure used to generate this phase space density, is an appealing feature of the ASW scheme from the perspective of quasiclassical dynamics calculations, which prevents spurious oscillations of time-dependent observables. We note again that the exact Wigner function remains invariant only under fully quantum mechanical propagation, exhibiting spiral fluctuations during classical evolution.[18a,23] Figure 7 also shows that the average potential arising from the harmonic-based Wigner density exhibits significant oscillations during classical trajectory propagation.

Time propagation is often used to generate spectra. Quantum ZPE effects are very important if the forces on the classical trajectories are obtained from *ab initio* electronic structure calculations, thus the use of a quantized phase space distribution is critical in this task. Below we discuss the quasiclassical time autocorrelation functions for the six normal modes of the modified formaldehyde potential, along with the corresponding mode-specific spectra.

The quantum mechanical position autocorrelation function for a normal mode is given by

$$C_k(t) = \mathrm{Tr}(\hat{\rho}_0 \hat{Q}_k(0) \hat{Q}_k(t)) \tag{3.5}$$

We use the primitive quasiclassical expression

$$\mathrm{Re}G_k(t) = \int_{-\infty}^{\infty} dQ_1(0) \cdots \int_{-\infty}^{\infty} dQ_n(0) \int_{-\infty}^{\infty} dP_1(0) \cdots \int_{-\infty}^{\infty} dP_n(0) W(Q_1(0), \ldots, Q_n(0), P_1(0), \ldots, P_n(0)) Q_k(0) Q_k(t) \tag{3.6}$$

DOI: 10.1021/acs.jctc.8b00179
J. Chem. Theory Comput. 2018, 14, 5446−5458

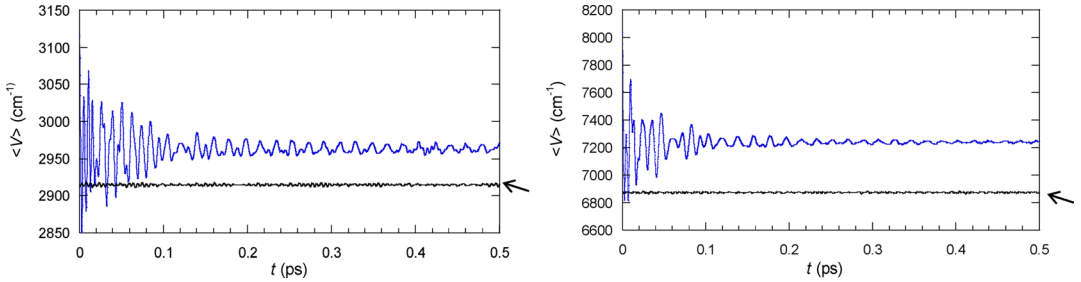

Figure 7. Average potential energy as a function of time. Blue line: harmonic Wigner density. Black line: ASW density. Left panel: T = 300 K, right: T = 3156 K. Arrow: the exact equilibrium value calculated by PIMC.

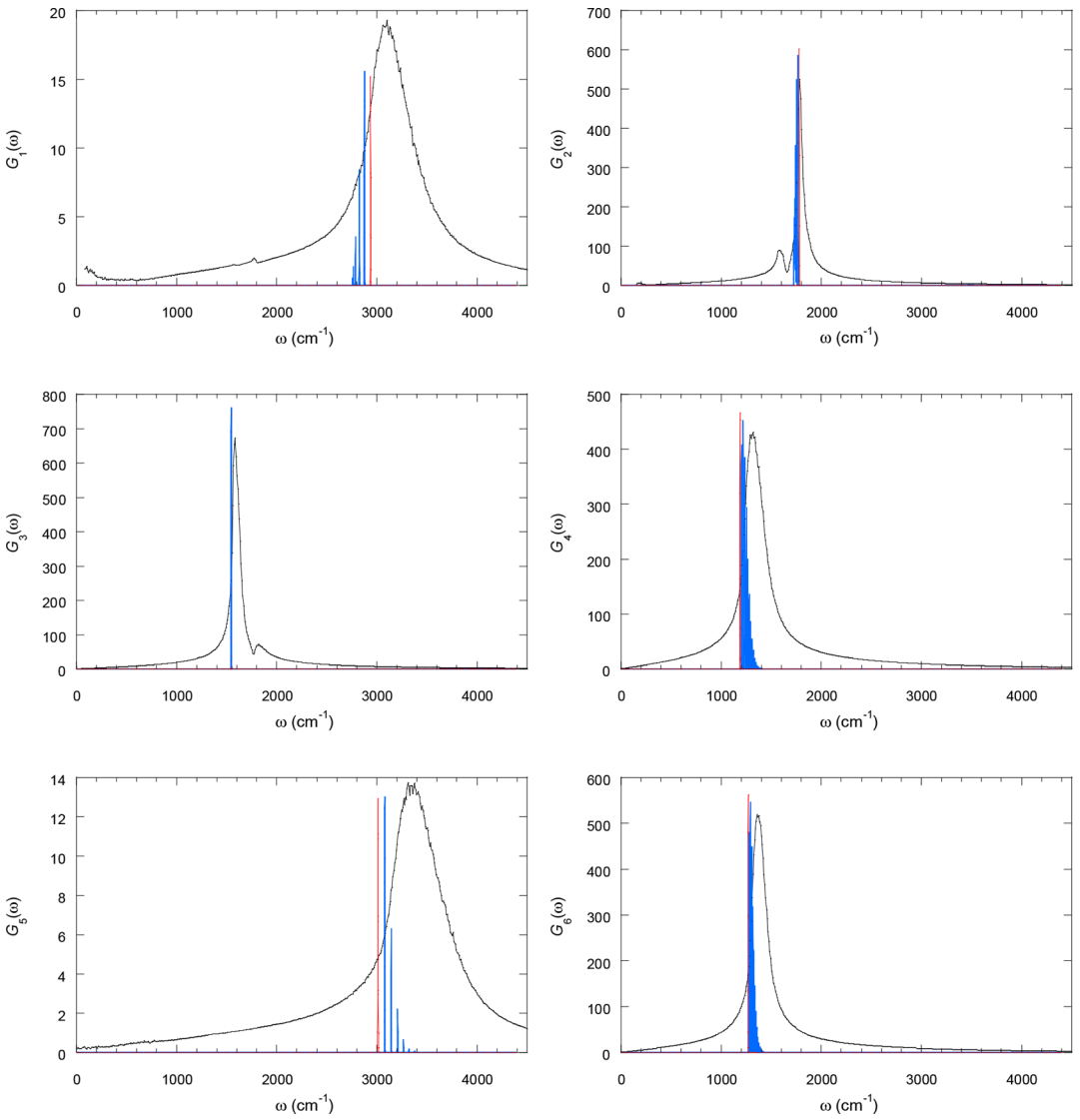

Figure 8. Mode-specific spectra at 3156 K obtained by Fourier transforming the position autocorrelation function of the six normal modes. Black lines show the spectra obtained from the quasiclassical procedure described in section II with the ASW density. Red lines indicate the quantum mechanical spectra arising from the harmonic part of the Hamiltonian. Blue lines show quantum mechanical results in the absence of anharmonic mode coupling terms. The relative peak heights in each set of stick spectra are correct, but the overall scaling is arbitrary.

to obtain the real part of the autocorrelation function, which we transform to the frequency domain, and use the procedure described in section II.2 to obtain the odd component of the spectrum which corresponds to the imaginary part of the autocorrelation function. This procedure yields the mode-specific spectra $G_k(\omega)$ within the quasiclassical approximation with the ASW density.

Figure 8 shows the mode-specific spectra obtained from the quasiclassical autocorrelation function, eq 2.5, at 3156 K. In addition, Figure 8 shows quantum mechanical spectra within the harmonic approximation and also with diagonal anharmonicity terms included (obtained from one-dimensional basis set calculations). The one-dimensional anharmonic spectra consist of delta functions (which have been given

DOI: 10.1021/acs.jctc.8b00179
J. Chem. Theory Comput. 2018, 14, 5446−5458

very small widths for visual clarity) whose peaks exhibit small, primarily blue shifts from the harmonic frequencies, which arise from the quartic potential terms.

The spectra shown in Figure 8 are significantly asymmetric through the addition of the odd spectral component to the even part obtained from the real part of the correlation function. This effect cannot be seen in Figure 8, since only the positive frequency axis is shown there. To illustrate this distortion, we show in Figure 9 the even and odd components,

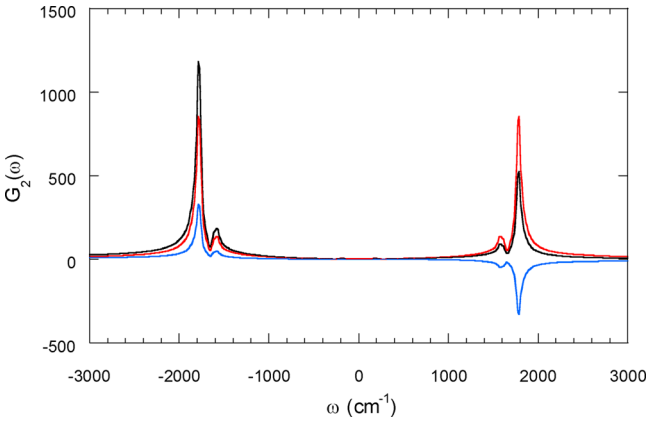

Figure 9. Quasiclassical ASW spectrum for normal mode 2 over the entire frequency domain. Red and blue lines show the even and odd components, respectively, while the black line shows the total spectrum.

along with the total spectrum over the entire frequency domain, for normal mode 2. The asymmetry which arises from the imaginary part of the autocorrelation function (which we obtain indirectly) is a strictly quantum mechanical effect and is prominent at fairly high temperatures in modes with relatively high frequencies. The effect is even more prominent in the higher frequency normal modes.

A fully quantum mechanical calculation of the correlation functions with all six coupled degrees of freedom would be illuminating but is rather challenging. However, we have been able to obtain accurate energy eigenvalues for several low-lying states via the original semiclassical adiabatic switching method.[13,22] The transition frequencies obtained from these values are shown in Figure 10. These transition frequencies

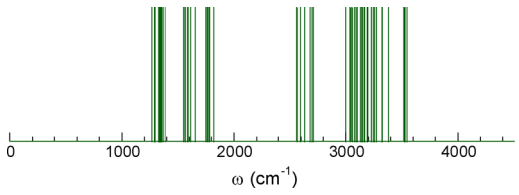

Figure 10. Transition frequencies from semiclassical eigenstates obtained via the ASW method.

exhibit additional blue shifts in comparison with those obtained from the calculations that account only for diagonal anharmonicity, a consequence of confining quartic terms in the mode−mode potential interactions. The spectral peaks obtained from the quasiclassical correlation functions with the ASW phase space density correlate well with the transition frequencies corresponding to the full six-dimensional potential. In addition, the ASW spectra are broadened. This broadening is an intrinsic feature of quasiclassical correlation functions, which eventually decay to zero without being able to account for recurrences associated with quantum interference. In very small systems of only a few degrees of freedom, the absence of recurrences and resulting spectral broadening tend to lead to significant discrepancies from fully quantum mechanical results. However, the rapidly growing number of transitions in polyatomic molecular systems causes very long recurrence times and densely packed spectral lines that are discernible only via high-resolution spectroscopic tools. In such situations quasiclassical calculations tend to produce a low-resolution spectrum that can offer adequate accuracy, provided that ZPE is properly accounted for in the phase space density that specifies trajectory initial conditions. The results presented in this section suggest that the ASW procedure provides an excellent way of achieving this quantization for molecular systems in the normal mode representation.

IV. APPLICATION TO BUTYNE DESCRIBED BY A CHARMM FORCE FIELD IN CARTESIAN COORDINATES

In this section we describe the application of the ASW method to a molecular Hamiltonian in Cartesian coordinates. The chosen system is the but-2-yne molecule, with intramolecular interactions described by the CHARMM force field.[24] Because they are parametrized to experimental observable, classical force fields account (approximately, in an average way) for some nuclear quantum effects at a particular temperature. It is thus clear that such force fields are meant to be used in classical molecular dynamics simulations with trajectories sampled from the classical Boltzmann distribution. Quantizing this distribution via a Wigner function would be double-counting quantum effects, which is likely to lead to worse results. Our goal in this study is to assess the consequences of density quantization on a typical small polyatomic molecule. We find the effects of this quantization to be rather large. Further, since the AS-Wigner approach allows efficient generation of the quantized Wigner density in the context of a classical trajectory simulation, it offers a practical way of reparameterizing force fields, making them suitable for molecular dynamics simulations with quantized initial conditions. This approach would capture quantum effects associated with nuclear zero-point energy and vibrational level structure faithfully, in full atomistic detail, over a wide range of temperatures.

The CHARMM potential is given in terms of bond lengths and angles, as well as nonbonded interactions. The latter consist of van der Waals interactions, which have the Lennard-Jones form, and Coulombic electrostatic interactions. All the parameters have been obtained from the CHARMM force field. The bond vibrations are described as purely harmonic vibrations. Thus, the anharmonicity in the Hamiltonian comes from the angular interaction terms, the Lennard-Jones form, and the electrostatic interactions.

Consider the molecule at room temperature (T = 298 K) and an elevated temperature of 400 K. The convergence of the potential energy distribution was used to determine a switching time of τ = 0.25 ps. Figure 11 shows the bond length distributions of the three unique types of bonds present in butyne, a CC single bond, a CH single bond, and a CC triple bond. We see that the exact quantum bond length distributions are quite faithfully reproduced by ASW. For the CC single and triple bonds, the method reproduces the PIMC results

DOI: 10.1021/acs.jctc.8b00179
J. Chem. Theory Comput. 2018, 14, 5446−5458

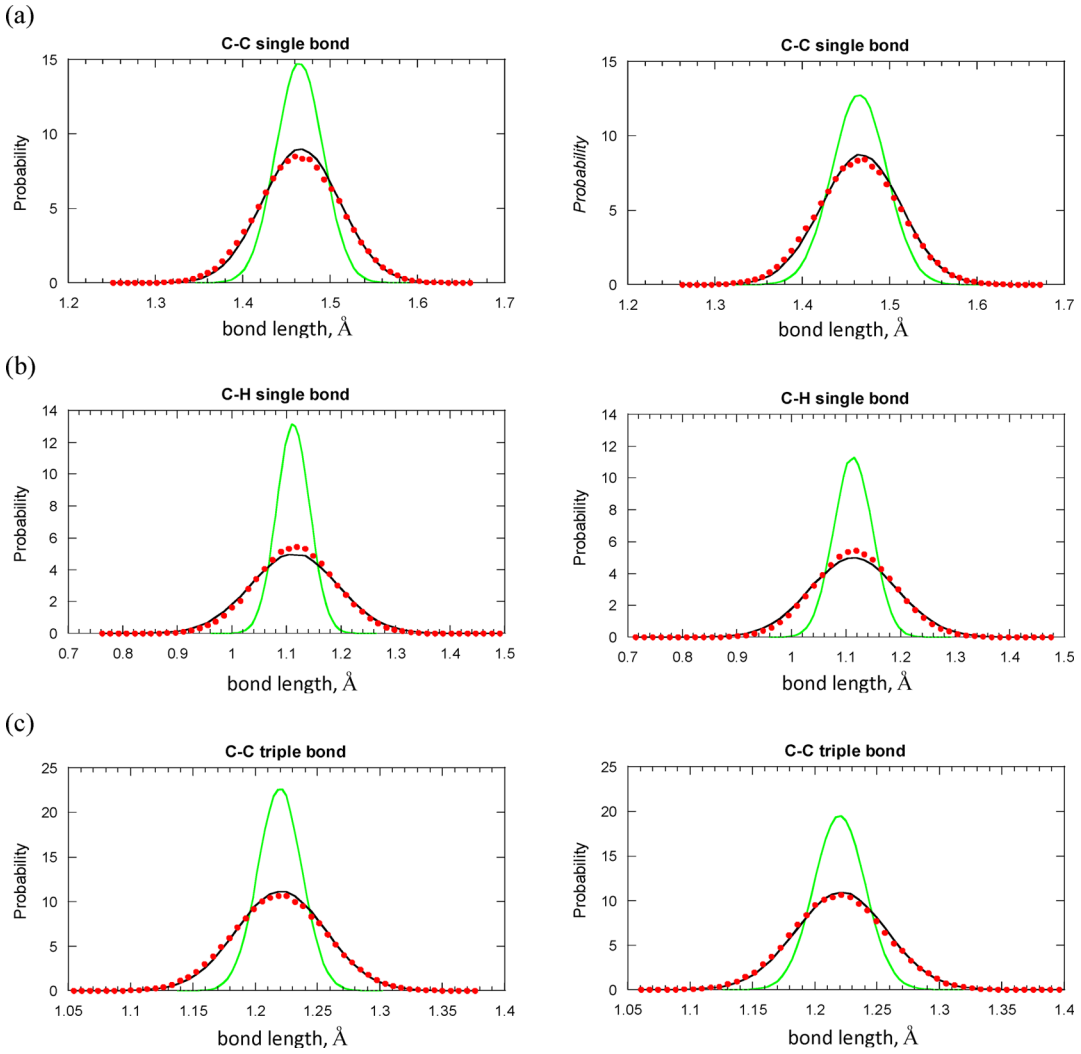

Figure 11. Distributions of bond lengths of the three different bonds at T = 298 K (left panels) and T = 400 K (right panels). Black line: PIMC results. Green line: classical Boltzmann approximation. Red markers: ASW results. Row (a): bond length distribution for CC single bonds, row (b): CH single bonds, row (c): CC triple bonds.

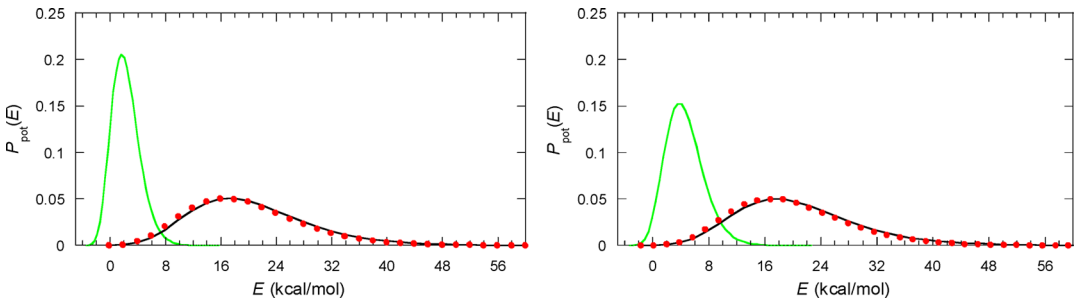

Figure 12. Distributions of bond lengths of the three different bonds at T = 298 K (left panel) and T = 400 K (right panel). Black line: PIMC results. Green line: classical Boltzmann approximation. Red markers: ASW results.

quantitatively. For the CH single bond, there are very slight differences between the PIMC and the ASW calculations, which occur because of errors accumulating over the many transformations to and from the Cartesian and normal mode coordinates. All the thermodynamic features of a quantum mechanical distribution are preserved in the ASW distributions. The classical distributions get broader on increasing the temperature, whereas both the PIMC and the ASW distributions remain invariant between temperatures of 298 K (left panels) and 400 K (right panels). This is indicative of the presence of zero point energy, and for this case of double quantization, at these temperatures, only the ground state is populated. The quantum mechanical excited state is not thermally accessible even at 400 K.

Figure 12 shows the potential energy distributions under the classical Boltzmann distribution and the quantum distributions at two different temperatures, 298 and 400 K, given by eq 3.2. We note that the ASW result matches the quantum PIMC

DOI: 10.1021/acs.jctc.8b00179
J. Chem. Theory Comput. 2018, 14, 5446−5458

results in a quantitative manner. The classical Boltzmann result undergoes a large change as the temperature is increased from 298 to 400 K, and the average potential energy shifts from 2.26 to 4.60 kcal/mol. The spread of the distributions also increases, from 2.01 to 2.70 kcal/mol. This is a consequence of the absence of ZPE in the classical density. By contrast, there is no such shift or broadening in either the PIMC or the ASW distribution. The ZPE effects shift the average potential energy up to almost 20 kcal/mol. The spread, though invariant with temperature, is still significantly greater than that in the purely classical simulation as a result of quantum penetration into classically forbidden regions of phase space.

V. CONCLUDING REMARKS

In this paper we have shown that the ASW method can be straightforwardly applied to generate the Wigner phase space density for a molecular system with several degrees of freedom whose potential function is available either in normal mode coordinates or in Cartesian coordinates. The implementation of the method is very simple in both cases; however, there are a few subtleties when the method is implemented in Cartesian coordinates. The starting Wigner density has a particularly simple form for the separable, quadratic normal mode zeroth-order Hamiltonian. Because the ASW procedure requires classical trajectory propagation, the potential energy function must be bound over the energy region accessed by trajectories whose initial conditions are sampled from the Wigner distribution of the quadratic normal mode Hamiltonian at the given temperature. This requirement is not particularly restrictive, given that the Wigner distribution is usually desired as the starting point of quasiclassical trajectory calculations, which would be subject to the same confining potential considerations.

A common use of the Wigner density is in the context of quasiclassical trajectory calculations. We have shown that dynamical properties can be obtained in a single procedure that involves classical trajectories sampled from the zeroth-order Wigner density, which are integrated first under the adiabatically switched potential and subsequently by the full Hamiltonian. Thus, the ASW method provides a very simple approach to quasiclassical calculations.

In its simplest form, which involves the Wigner transform of the bare Boltzmann factor, the quasiclassical expression is real valued, thus this procedure cannot give the imaginary part of time correlation functions which leads to distortion of the spectrum. We have shown that the spectral component corresponding to the imaginary part can be inferred, thus prominent features of molecular spectra are accurately accounted for.

We first applied the ASW method to the formaldehyde molecule in the normal mode representation, with a small modification of the anharmonic terms to prevent unbound trajectories. A number of comparisons against highly accurate PIMC calculations demonstrated that the ASW procedure yields a highly accurate quantum phase space distribution over a wide range of temperatures. In order to provide a challenge to the ASW method, we included temperatures that are unrealistically high for this molecule but are such that cause the trajectories to access regions of strong anharmonicity; such regions would be accessible at physiological temperatures in large molecules containing many low-frequency vibrations. Simple harmonic approximations to the Wigner density cannot describe such anharmonic regions properly, while the classical Boltzmann distribution is unable to account for ZPE effects and thus fails at low temperatures. Given the quadratic nature of the reference Hamiltonian, which is the starting point for the ASW procedure, the strongly anharmonic, high-temperature regime is most challenging, thus the ability of the ASW procedure to yield highly accurate results in this regime is very encouraging.

As a second example of calculating the quantum phase space distribution for an atomistic potential, we applied it to the butyne molecule described by the CHARMM force field. In this case, of course, the quantization leads to a double inclusion of the quantum effects; however, it is sufficient as a test of correctness and applicability of the ASW method for Hamiltonians in Cartesian coordinates. The most attractive feature of using the ASW procedure with ab initio potential energy surfaces even in the Cartesian coordinates stems from the fact that the method is no longer limited to a certain parameter regime of fitting. In fact, it would be very exciting to couple this method to density functional theory or other electronic structure methods which can give us the locally relevant Born−Oppenheimer potential energy surface on the fly.

When used for launching classical trajectories, the ASW density has the desirable feature of exactly preserving the temporal invariance of the distribution, thus eliminating spurious oscillatory features in dynamical observables. Quasiclassical trajectory calculations often provide the only pragmatic approach to time-dependent properties of polyatomic systems. However, if accurate *ab initio* potential energy calculations are employed for force determination, it is necessary to account for quantum mechanical effects in the initial phase space distribution. The ASW scheme is ideally suited to this task. It yields highly accurate results with relatively little effort and requires practically no additional setup, as the trajectories used to generate it can be continued forward in time in order to generate the desired dynamics. We thus envision that the ASW will find broad application in the simulation of molecular systems via quasiclassical methods. It will be most interesting to apply the ASW procedure to larger molecular systems whose intramolecular dynamics are described by accurate, permutationally invariant potential energy surfaces[25] that do not lead to unbound trajectories.

Quasiclassical trajectory calculations produce time correlation functions that tend to decay faster than their fully quantum mechanical counterparts, giving rise to broadened spectra. This artifact is not a severe flaw in systems of many degrees of freedom, where the density of spectral lines is high and individual peaks can be distinguished only via high resolution spectroscopy. A recently proposed imaginary-time path integral-based Liouville dynamics (PILD) method,[26] which can be derived from equilibrium Wigner dynamics,[27] has been shown to remove much of this broadening, capturing sharp spectral peaks even with less accurate Gaussian approximations to the Wigner density. Combination with the ASW approach to generate a more accurate phase space density for PILD propagation may lead to a very promising and practical approach for generating quasiclassical spectra in small polyatomic molecules.

Last, the ASW procedure may be applied without modification to generate a quantized phase space distribution in a subspace of the system's coordinates, as required in the quantum-classical path integral (QCPI) methodology.[28] QCPI offers a rigorous quantum-classical description of nonadiabatic

DOI: 10.1021/acs.jctc.8b00179
J. Chem. Theory Comput. 2018, 14, 5446−5458

processes in condensed phase and biological environments which captures the interaction between quantum and classical degrees of freedom without *ad hoc* assumptions or approximations. Recent applications to charge transfer processes in solution (where over 1000 solvent degrees of freedom were described by classical trajectories governed by classical force fields while the charge transfer pair was treated fully quantum mechanically via the path integral formulation[29]) showed that accurate, assumption-free quantum-classical simulations are within reach. More recent developments[30] have increased dramatically the efficiency of the QCPI methodology, allowing highly accurate calculations with effort comparable to that in routine molecular dynamics simulation. These developments invite application of QCPI to charge transfer in materials, where classical force fields are not available, thus *ab initio* evaluation of the forces offers the only available avenue. However, ZPE effects in vibrational degrees of freedom are expected to be large. The ASW methodology will allow quantization of the phase space density describing the nuclear degrees of freedom within the QCPI framework, providing a highly accurate and efficient approach to charge transfer processes in many condensed phase systems.

AUTHOR INFORMATION

Corresponding Author

*E-mail: nmakri@illinois.edu.

ORCID

Amartya Bose: 0000-0003-0685-5096

Nancy Makri: 0000-0002-3310-7328

Funding

This material is based upon work supported by the National Science Foundation under Award CHE-1665281.

Notes

The authors declare no competing financial interest.

REFERENCES

(1) (a) Wigner, E. J. Calculation of the Rate of Elementary Association Reactions. *J. Chem. Phys.* **1937**, *5*, 720. (b) Heller, E. J.; Brown, R. C. Errors in the Wigner approach to quantum dynamics. *J. Chem. Phys.* **1981**, *75*, 1048−1050.

(2) (a) Wang, H.; Sun, X.; Miller, W. H. Semiclassical approximations for the calculation of thermal rate constants for chemical reactions in complex molecular systems. *J. Chem. Phys.* **1998**, *108*, 9726−9736. (b) Sun, X.; Wang, H.; Miller, W. H. Semiclassical theory of electronically nonadiabatic dynamics: Results of a linearized approximation to the initial value representation. *J. Chem. Phys.* **1998**, *109*, 7064−7074. (c) Miller, W. H. Generalization of the linearized approximation to the semiclassical initial value representation for reactive flux correlation functions. *J. Phys. Chem. A* **1999**, *103*, 9384−9387.

(3) Poulsen, J. A.; Nyman, G.; Rossky, P. J. Practical evaluation of condensed phase quantum correlation functions: A Feynman–Kleinert variational linearized path integral method. *J. Chem. Phys.* **2003**, *119* (23), 12179−12193.

(4) (a) Donoso, A.; Martens, C. C. Semiclassical multistate Liouville dynamics in the adiabatic representation. *J. Chem. Phys.* **2000**, *112*, 3980−3989. (b) Hsieh, C. Y.; Kapral, R. Nonadiabatic dynamics in open quantum-classical systems: Forward-backward trajectory solution. *J. Chem. Phys.* **2012**, *137*, 22A507. (c) Kapral, R. Quantum dynamics in open quantum-classical systems. *J. Phys.: Condens. Matter* **2015**, *27*, 073201.

(5) Metropolis, N.; Rosenbluth, A. W.; Rosenbluth, M. N.; Teller, H.; Teller, E. Equation of state calculations by fast computing machines. *J. Chem. Phys.* **1953**, *21*, 1087−1092.

(6) Shi, Q.; Geva, E. Semiclassical theory of vibrational energy relaxation in the condensed phase. *J. Phys. Chem. A* **2003**, *107*, 9059−9069.

(7) (a) Frantsuzov, P. A.; Neumaier, A.; Mandelshtam, V. A. Gaussian resolutions for equilibrium density matrices. *Chem. Phys. Lett.* **2003**, *381*, 117. (b) Frantsuzov, P. A.; Mandelshtam, V. A. Quantum statistical mechanics with Gaussians: Equilibrium properties of van der Waals clusters. *J. Chem. Phys.* **2004**, *121*, 9247.

(8) Heller, E. J. Time-dependent variational approach to semiclassical dynamics. *J. Chem. Phys.* **1976**, *64*, 63−73.

(9) Shao, J.; Pollak, E. A new time evolving Gaussian series representation of the imaginary time propagator. *J. Chem. Phys.* **2006**, *125*, 133502.

(10) Makri, N. Improved Feynman propagators on a grid and non-adiabatic corrections within the path integral framework. *Chem. Phys. Lett.* **1992**, *193*, 435−444.

(11) Montoya-Castillo, A.; Reichman, D. R. Path integral approach to the Wigner representation of canonical density operators for discrete systems coupled to harmonic baths. *J. Chem. Phys.* **2017**, *146*, 024107.

(12) Bose, A.; Makri, N. Evaluation of the Wigner distribution via classical adiabatic switching. *J. Chem. Phys.* **2015**, *143*, 114114.

(13) Ehrenfest, P. On adiabatic changes of a system in connection with quantum theory. *Verslagen Kon. Akad. Amsterdam* **1916**, *25*, 412.

(14) Romanowski, H.; Bowman, J. M.; Harding, L. B. Vibrational energy levels of formaldehyde. *J. Chem. Phys.* **1985**, *82*, 4155.

(15) (a) Fosdick, L. D.; Jordan, H. F. Path integral calculation of the two-particle Slater sum for He^4. *Phys. Rev.* **1966**, *143*, 58−66. (b) Lawande, S. V.; Jensen, C. A.; Sahlin, H. L. Monte Carlo integration of the Feynman propagator in imaginary time. *J. Comput. Phys.* **1969**, *3*, 416−443. (c) Bernu, B.; Ceperley, D. M. Path integral Monte Carlo. In *Quantum simulations of complex many-body systems: From theory to algorithms*, Grotendorst, J., Marx, D., Muramatsu, A., Eds.; John von Neumann Institute for Computing: 2002; Vol. *10*.

(16) Suzuki, M. *Quantum Monte Carlo methods in condensed matter physics*; World Scientific: Singapore, 1993; DOI: 10.1142/2262.

(17) Liu, J.; Miller, W. H. Real time correlation functions in a single phase space integral beyond the linearized semiclassial initial value representation. *J. Chem. Phys.* **2007**, *126*, 234110.

(18) (a) Liu, J.; Makri, N. Symmetries and detailed balance in forward-backward semiclassical dynamics. *Chem. Phys.* **2006**, *322*, 23−29. (b) Chen, J.; Makri, N. Forward-backward semiclassical dynamics with single-bead coherent state density. *Mol. Phys.* **2008**, *106*, 443.

(19) Eckart, C. Some Studies Concerning Rotating Axes and Polyatomic Molecules. *Phys. Rev.* **1935**, *47*, 552.

(20) Czakó, G.; Bowman, J. M. Reaction Dynamics of Methane with F, O, Cl, and Br on ab Initio Potential Energy Surfaces. *J. Phys. Chem. A* **2014**, *118*, 2839−2864.

(21) Sun, Q.; Bowman, J. M.; Gazdy, B. Application of adiabatic switching to vibrational energies of three-dimensional HCO, H2O and H2CO. *J. Chem. Phys.* **1988**, *89*, 3124−3130.

(22) (a) Skodje, R. T.; Borondo, F.; Reinhardt, W. P. The semiclassical quantization of nonseparable systems using the method of adiabatic switching. *J. Chem. Phys.* **1985**, *82*, 4611. (b) Skodje, R. T.; Cary, J. R. An analysis of the adiabatic switching method: Foundations and applications. *Comput. Phys. Rep.* **1988**, *8*, 221−292. (c) Zakrzewski, J.; Saini, S.; Taylor, H. S. Semiclassical quantization via adiabatic switching. I. Choice of tori and initial conditions for two-dimensional systems. *Phys. Rev. A: At., Mol., Opt. Phys.* **1988**, *38*, 3877−3899. (d) Saini, S.; Zakrzewski, J.; Taylor, H. S. Semiclassical quantization via adiabatic switching. II. Choice of tori and initial conditions for multidimensional systems. *Phys. Rev. A: At., Mol., Opt. Phys.* **1988**, *38*, 3900−3908. (e) Johnson, B. R. Semiclassical vibrational eigenvalues of H2O and SO2 by the adiabatic switching method. *Comput. Phys. Commun.* **1988**, *51*, 1−10.

(23) Wright, N. J.; Makri, N. Phase space and statistical aspects of forward-backward semiclassical dynamics. *J. Phys. Chem. B* **2004**, *108*, 6816−6825.

DOI: 10.1021/acs.jctc.8b00179
J. Chem. Theory Comput. 2018, 14, 5446−5458

(24) Vanommeslaeghe, K.; Hatcher, E.; Acharya, C.; Kundu, S.; Zhong, S.; Shim, J.; Darian, E.; Guvench, O.; Lopes, P.; Vorobyov, I.; MacKerell, A. D., Jr. CHARMM General Force Field: A Force Field for Drug-Like Molecules Compatible with the CHARMM All-Atom Additive Biological Force Fields. *J. Comput. Chem.* **2010**, *31*, 671−690.
(25) (a) Qu, C.; Bowman, J. M. An ab initio potential energy surface for the formic acid dimer: zero-point energy, selected anharmonic fundamental energies, and ground-state tunneling splitting calculated in relaxed 1−4-mode subspaces. *Phys. Chem. Chem. Phys.* **2016**, *18*, 24835−24840. (b) Nguyen, T. T.; Szekely, E.; Imbalzano, G.; Behler, J.; Csanyi, G.; Ceriotti, M.; Gotz, A.; Paesani, F. Comparison of permutationally invariant polynomials, neural networks, and Gaussian approximation potentials in representing water interactions through many-body expansions. *J. Chem. Phys.* **2018**, *148*, 241725.
(26) (a) Liu, J. Path integral Liouville dynamics for thermal equilibrium systems. *J. Chem. Phys.* **2014**, *140*, 224107. (b) Liu, J.; Zhang, Z. Path integral Liouville dynamics: Applications to infrared spectra of OH, water, ammonia, and methane. *J. Chem. Phys.* **2016**, *144*, 034307.
(27) Liu, J.; Miller, W. An approach for generating trajectory-based dynamics which conserves the canonical distribution in the phase space formulation of quantum mechanics. I. Theories. *J. Chem. Phys.* **2011**, *134*, 104101.
(28) (a) Lambert, R.; Makri, N. Quantum-classical path integral: Classical memory and weak quantum nonlocality. *J. Chem. Phys.* **2012**, *137*, 22A552. (b) Lambert, R.; Makri, N. Quantum-classical path integral: Numerical formulation. *J. Chem. Phys.* **2012**, *137*, 22A553. (c) Makri, N. Quantum-classical path integral: A rigorous approach to condensed phase dynamics. *Int. J. Quantum Chem.* **2015**, *115*, 1209−1214.
(29) Walters, P. L.; Makri, N. Quantum-classical path integral simulation of the ferrocene-ferrocenium charge transfer in liquid hexane. *J. Phys. Chem. Lett.* **2015**, *6*, 4959−4965.
(30) Makri, N. Blip-summed quantum-classical path integral with cumulative quantum memory. *Faraday Discuss.* **2016**, *195*, 81−92.

DOI: 10.1021/acs.jctc.8b00179
J. Chem. Theory Comput. 2018, 14, 5446−5458